# Distribution and Effects of Gas Porosity in Welds in CVD Tungsten

## Three types of pore distribution are noted in the fusion zone and pore linkup in the heat-affected zone leads to the formation of heat-affected zone microfissures

BY C. D. LUNDIN AND K. FARRELL

### Introduction

New techniques are constantly being developed for the production and fabrication of metals and alloys. One of these techniques, chemical vapor deposition,[1-2] abbreviated to CVD, is fully recognized as an attractive way of directly producing complex shapes as well as a means of obtaining quality base metal for further fabrication. Although other methods[3] have been used to join CVD alloys, fusion welding is still the most satisfactory method. But, as this paper demonstrates, fusion welding of CVD refractory metals may lead to problems not previously encountered in the more conventional high-purity refractory metals.

CVD tungsten is produced by hydrogen reduction of $WF_6$ vapor to deposit metallic tungsten on a heated substrate[4] through the reaction:

$$WF_6(g) + 3H_2(g) \xrightarrow{1200^\circ\ F} W(s) + 6HF(g)$$

The deposited tungsten takes the shape of the substrate. Growth of the CVD tungsten from the substrate is crystallographically controlled once a small amount of tungsten is deposited. Preferred growth takes place in which columnar grains grow with their <100> crystallographic axes normal to the substrate. Figure 1 shows a polished and etched section through a 0.070 in. thick CVD tungsten sheet. The substrate was originally at the bottom and growth proceeded upwards. Note the highly irregular or "jagged" grain boundaries separating the columnar grains. This structure is typical of as-deposited CVD material.

Previous studies[5-7] of the annealing response of CVD tungsten have shown that gas porosity develops in it during high-temperature annealing. Growth of such pores under an applied stress[8, 9] adversely affects the creep rupture properties of the material. Figure 2 shows such pores developed on the grain boundaries. The boundaries have now lost the jagged appearance, and fracture is likely to occur along the grain boundaries through the pores. In addition, the pores will link up to cause gross grain-boundary fissuring and eventual fracture during high-temperature stress-rupture tests.[8, 9] The pores are believed to be nucleated from dissolved gases and lattice vacancies present in the as-deposited material and to grow preferentially on the grain boundaries by diffusion processes during elevated temperature exposure. Growth of the pores is enhanced by tensile stresses.[8,9]

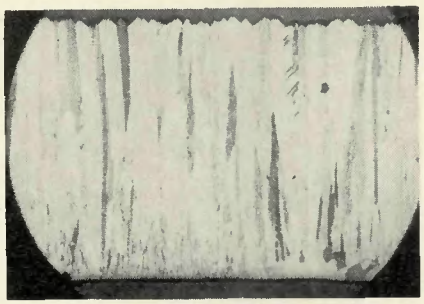

Fig. 1—Cross section of 0.070 in. thick CVD sheet. Etched with $H_2O_2$-$NH_4OH$. X50 (reduced 60% on reproduction)

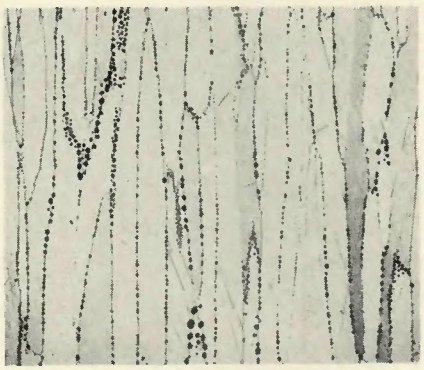

Fig. 2—CVD tungsten after high-temperature anneal. Etched with $H_2O_2$-$NH_4OH$. X100 (reduced 50% on reproduction)

Fusion welding of CVD tungsten necessarily involves exposure to a range of temperatures from the initial plate temperature to above the melting point. Also, thermally induced and restraint-induced stresses are set up. Under these combined effects, pore nucleation and growth can be expected. This paper illustrates some of our observations on the development and behavior of gas porosity in fusion welds in CVD tungsten.

### Materials

We used 0.070 in. thick CVD sheet. A typical composition (ppm by weight) for this material is C, < 20; O, 14; N, 1; H, 1; and F, 20. This composition is typical of most high-purity tungsten regardless of the processing history with the exception of fluorine, which is a carryover from the CVD process.

### Welding Procedure

Full and partial penetration welds were made by the gas tungsten-arc and the electron-beam processes from the top of the CVD sheets. The sheets were fully restrained in a copper fixture during welding. Argon shielding gas was used for the gas tungsten-arc welds, and the dcsp current, voltage, and travel speed were varied.

### Metallography

Optical metallography was carried

C. D. LUNDIN is a Consultant from the University of Tennessee and K. FARRELL is with the Metals and Ceramics Div., Oak Ridge National Laboratory, Oak Ridge, Tenn.

Paper presented at the AWS 51st Annual Meeting held in Cleveland, Ohio, during June 8-12, 1970.

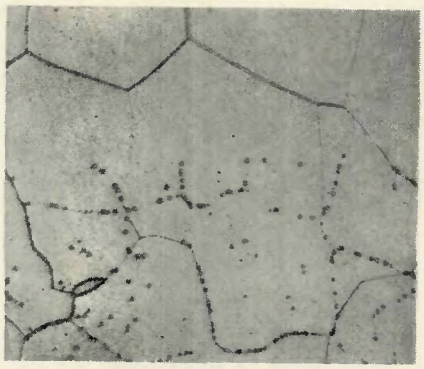

Fig. 3—Fusion line of a gas tungsten-arc weld in CVD tungsten. Etched with $H_2O_2$-$NH_4OH$. X500 (reduced 50% on reproduction)

out on polished and etched weld sections. Specimens were etched with a mixture of equal volumes of $H_2O_2$ and $NH_4OH$. Careful etching is necessary since tungsten will etch-pit easily and this etch pitting, if not recognized, will confuse the results.

Some welds were fractured at room temperature to expose pores and grain boundaries for examination. These features were studied by electron fractographic techniques using direct carbon replicas of the surfaces. Such studies enabled fine detail to be observed. Where detail was less important than ability to examine the whole area of the fractured welds, scanning electron microscopy was employed.

## Results and Discussion

The distribution of porosity in the heat-affected zone and the fusion zone were quite different and are best discussed separately.

### Porosity in the Heat-Affected Zone

Figure 3 shows the distribution of pores in the heat-affected zone and

Fig. 4—Fissures produced by pore link-up in arc-welded CVD tungsten. X500 (reduced 50% in reproduction)

fusion zone of a gas tungsten-arc weld in CVD tungsten. The size of the pores in the heat-affected zone decreases as we move into the base metal away from the fusion line. The

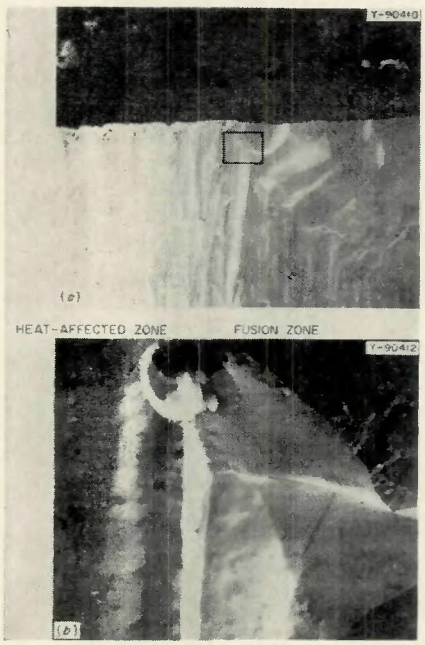


Fig. 5—Scanning electron micrographs of fracture surface of partial penetration weld in CVD tungsten. (a) X100; (b) X1000 (reduced 54% on reproduction)

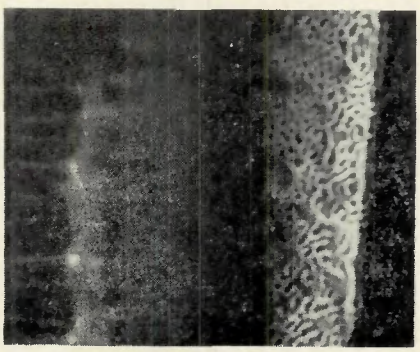

Fig. 6—Scanning electron micrograph of heat-affected zone in welded CVD tungsten. "Wormholes" result from link-up of pores. X3000 (reduced 46% on reproduction)

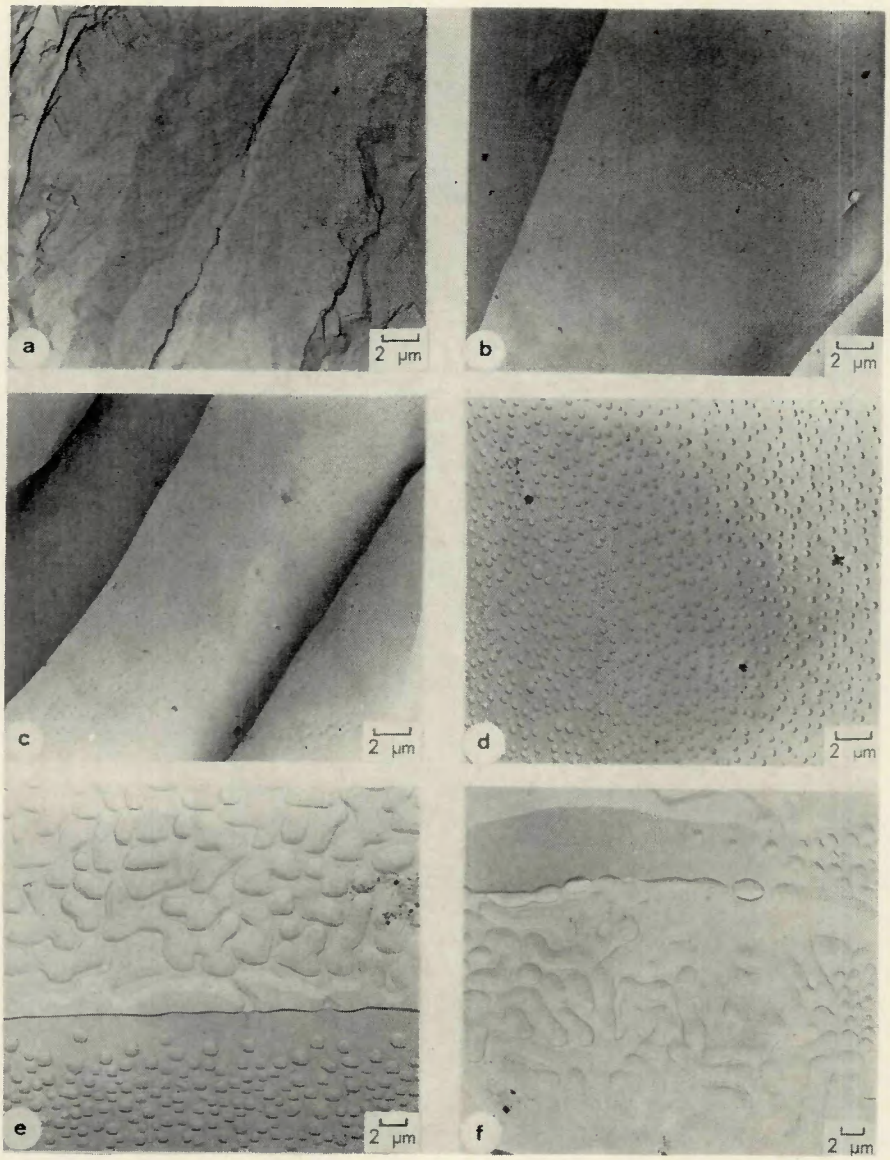


Fig. 7—Fractographs of grain boundaries in as-deposited CVD tungsten: (a) base metal, X3400; (b) heat-affected zone farthest from weld, X3400; (c) heat-affected zone about 1 mm from fusion line, X3400; (d) heat-affected zone nearest fusion line, X3400; (e) (f) heat-affected zone almost at fusion line, (e) X2600, (f) X2300 (reduced 32% on reproduction)

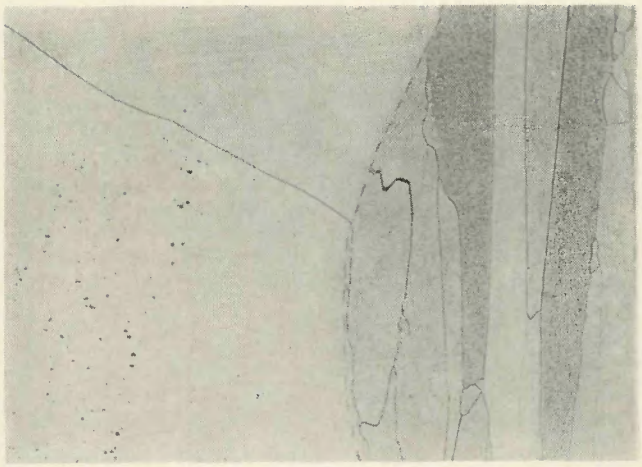

Fig. 8—Cross section of arc weld in CVD tungsten. Fusion zone is to the left of the dashed line and heat-affected zone to the right. Etched with $H_2O_2$-$NH_4OH$. X200 (reduced 45% on reproduction)

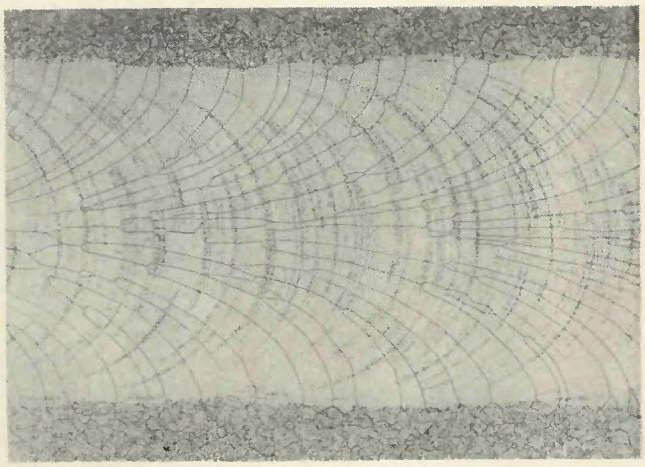

Fig. 9—Top surface view of electron-beam weld in CVD tungsten. Polished and etched with $H_2O_2$-$NH_4OH$. X100 (reduced 45% on reproduction)

distribution of the pores illustrates the preferential pore formation on grain boundaries. These pores pin the grain boundaries and usually prevent grain growth. But at the fusion line the temperature reaches a maximum for the heat-affected zone, and some grain boundary migration occurs. The pores left behind by the moving boundaries can clearly be seen. The fusion zone, at the top in Fig. 3, contains fewer and smaller pores than the heat-affected zone.

In many instances the pores on the heat-affected zone grain boundaries link up and form a continuous fissure along the boundary. When this occurs, the properties of the welded structure are seriously degraded. This linkup of pores to form fissures is illustrated by Fig. 4. In this micrograph the fusion zone is at the right and the heat-affected zone at the left. Fractographic studies of welds exhibiting this behavior confirm that the grain boundary fissures form from coalescence of pores. Figure 5 shows scanning electron micrographs of the fracture surface of a partial penetration weld in CVD tungsten. Figure 5(a) at X100 clearly shows the fusion zone and heat-affected zone grain size and shape. The X1000 micrograph in Fig. 5(b) from the outlined area in Fig. 5(a) shows the pores along the fusion zone and heat-affected zone grain boundaries. The difference in the number of pores on each side of the fusion line agrees with the conventional optical metallographic observations. Figure 6 is a scanning micrograph at X3000 of another heat-affected zone location showing linkup of the pores to form "wormholes."

Examination of fracture replicas from the welds reveals pore coalescence in more detail. The fractographs in Fig. 7 represent various locations in the weld heat-affected zone. Figure 7(a), from the base metal, illustrates jagged boundaries devoid of pores. As the fusion line is approached [micrographs (b) through (f)] the grain boundaries are smoothed out and the development of fine porosity becomes evident. In micrographs (e) and (f), adjacent to the fusion zone, pore linkup is well established.

This process of pore coalescence has been considered in detail in an earlier paper,[10] which contended that this is the mechanism of hot cracking in fusion welds in a number of grades of tungsten, including the arc-melted grade. This is one instance of hot cracking where a liquid film is not involved. We have also found extensive gas porosity in welds in electrodeposited nickel and iron.

### Porosity in the Fusion Zone

The porosity in the fusion zone bore little or no resemblance to that in the heat-affected zone. The incidence of grain boundary porosity was much less in the fusion zone, and no cases of grain boundary pore coalescence were found.

Three classes of pores existed in the fusion zone. The most obvious of these was what we will call "gross" porosity. This usually occurred at the bottom of the weld pool and consisted of an

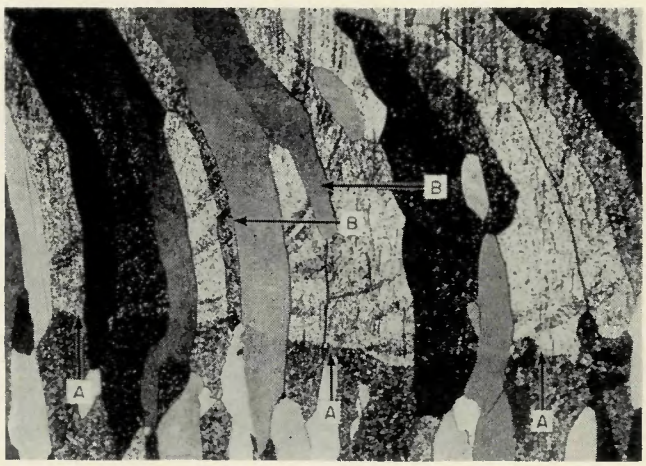


Fig. 10—Longitudinal cross section along center line of the weld shown in Fig. 9. Etched with $H_2O_2$-$NH_4OH$. Arrows A show root of weld, and B shows ripple markings extending to top. X100 (reduced 33% on reproduction)

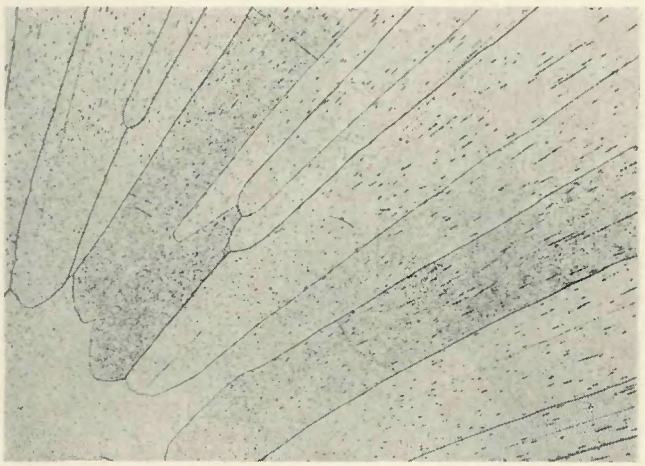

Fig. 11—Weld fusion zone. The pore distribution indicates preferential formation parallel to the axis of columnar grains. Etched with $H_2O_2$-$NH_4OH$. X200 (reduced 49% on reproduction)

irregular collection or pocket of large pores, as shown on the left in Fig. 8. We believe that this porosity is related to that in the heat-affected zone in that these pores grew mostly in the solid state during the heating half of the weld cycle. When fusion occurred the pores would be compelled to rise through the liquid pool like gas bubbles. Some pores would touch and coalesce and grow quite large—Fig. 4, upper right. Those close to the top surface of the pool would escape, but those from the underside of the pool would be trapped in the lower sections of the pool during solidification, forming the pockets that we observed. The location of these pockets appeared to be influenced more by the weld pool shape than by any single weld parameter.

The other two classes of porosity in the fusion zone were on a much finer scale than the gross porosity. In fact, the pores were so small that we had to etch the specimens quite strongly to excavate the pores and reveal their locations more clearly. This fine porosity is probably caused by rejection of excess dissolved gases from the weld pool during solidification. This porosity is illustrated in Figs. 9 through 11.

Figure 9 is a polished and etched top surface view of a partial-penetration electron-beam weld made at a travel speed of 35 ipm. The weld progressed from right to left as shown in this micrograph, and the porosity delineates the weld ripple pattern. This decoration of the weld ripples by the pores suggests that the formation of the pores is related to the motion of the weld pool, since the ripples are known to mark instantaneous locations of the weld pool during its travel along the plate. This phenomenon has been noted by others primarily in aluminum alloys, and the same "nucleation from the melt" phenomena undoubtedly prevail. This decoration process extended also to the root of the weld.

Figure 10, a longitudinal section of the weld shown in Fig. 9, illustrates this behavior. One can clearly see the scalloped root of the weld (Arrow A) and the curved sweep of the ripple markings (Arrow B) extending toward the top of the weld. This ripple-pore pattern indicative of the weld progression did not appear to cause any unusual mechanical property behavior nor was it related in any way to weld failure.

Close examination of Fig. 10 also reveals another characteristic pore distribution, one in which the pores tend to line up along the axis of the grains. This is perhaps best illustrated in Fig. 11. Although no solidification substructure is visible, gas pores have

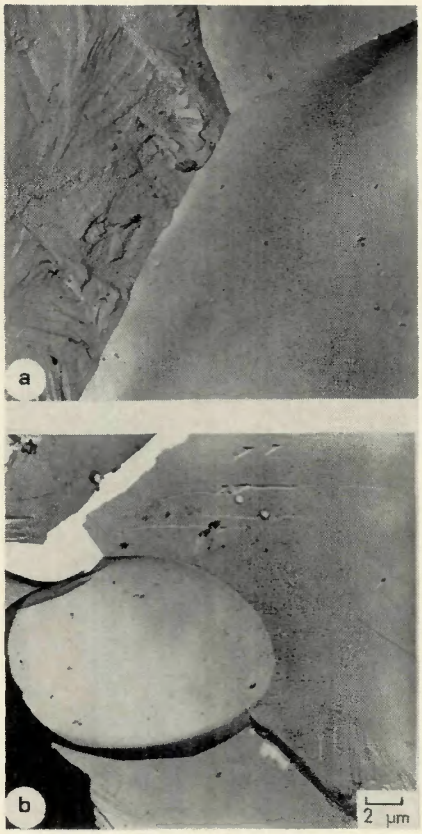


Fig. 12—Pores in weld bead in as-deposited CVD tungsten. (a) On grain boundaries; (b) within grains. X3400 (reduced 33% on reproduction)

apparently deposited preferentially in much the same manner as segregation would in a cellular mode of weld metal growth. Again this pore distribution did not appear to influence weld failure characteristics.

The weld ripple-related and solidification-related pore distributions both occurred more readily in welds that experienced steep temperature gradients and high solidification rates. Thus the electron-beam welds and higher travel speed gas tungsten-arc welds exhibited this behavior.

None of the pores in the fusion zone appeared to have any relationship to weld failure characteristics. Electron fractographic studies of these pores revealed that the few pores on grain boundaries were isolated and showed no apparent tendency to link up or grow together. An electron fractograph showing the pores on grain boundaries in the fusion zone is shown in Fig. 12(a). Figure 12(b) shows one of the large pores within a grain.

## Conclusions

1. Extensive gas porosity was found in the heat-affected zone and fusion zone of fusion welds in CVD tungsten.

2. Pores were observed to nucleate and grow on grain boundaries in the heat-affected zone. The extent of pore growth depended upon the weld thermal cycle and on whether or not grain boundary migration occurred.

3. Pore linkup in the heat-affected zone was observed in many instances, leading to the formation of heat-affected zone microfissures.

4. Three types of pore distributions were noted in the fusion zone. Two of these, involving very small pores, were clearly associated with weld pool motion and solidification, and are believed to result from precipitation of dissolved gases during solidification of the weld pool. The remainng porosity was on a large scale and was thought to be due to entrapment of gas pores that existed before melting occurred.

*Acknowledgements*

The authors acknowledge Nancy C. Cole and G. M. Slaughter for helpful discussions, E. R. Boyd for metallography, and A. L. Coffey and R. Bennett of the Y-12 Plant for scanning electron microscopy

The research described in this paper was sponsored by the U.S. Atomic Energy Commission under contract with Union Carbide Corporation.

*References*

1. Powell, C. F., Oxley, J. H., and Blocher, J. M., Jr., eds., *Vapor Deposition*, John Wiley & Sons, Inc., New York, 1966.

2. Schaffhauser, A. C., ed., *Proceedings of Conference on Chemical Vapor Deposition of Refractory Metals, Alloys, and Compounds, Gatlinburg, Tennessee, September 12-14, 1967*, American Nuclear Society. Hinsdale, Ill., 1967.

3. Wilson, R. W., "Chemical Vapor Deposition Welding—Below the Recrystallization Temperatures," WELDING JOURNAL, 47 (8), Research Suppl., 345-s to 354-s (1968).

4. Heestand, R. L., Federer, J. I., and Leitten, C. F., Jr., *Preparation and Evaluation of Vapor-Deposited Tungsten*, Report ORNL-3662, Oak Ridge National Laboratory, August 1964.

5. Schaffhauser, A. C., and Farrell, K., "Gas Bubbles in Thermochemically Deposited Tungsten," *Journal of Nuclear Materials*, 22 (1), 106-108 (1967).

6. Farrell, K., Houston, J. T., and Schaffhauser, A. C., "The Growth of Grain-Boundary Gas Bubbles in Chemically Vapor Deposited Tungsten," pp. 363-390 in *Proceedings of Conference on Chemical Vapor Deposition of Refractory Metals, Alloys, and Compounds, Gatlinburg, Tennessee, September 12-14, 1967*, American Nuclear Society, Hinsdale, Ill., 1967.

7. Farrell, K., Loh, B. T. M., and Stiegler, J. O., "Morphologies of Bubbles and Voids in Tungsten," *ASM Transaction Quarterly*, 60 (3), 485-493 (1967).

8. McCoy, H. E., and Stiegler, J. O., "Mechanical Behavior of CVD Tungsten at Elevated Temperatures," pp. 391-425 in *Proceedings of Conference on Chemical Vapor Deposition of Refractory Metals, Alloys, and Compounds, Gatlinburg, Tennessee, September 12-14, 1967*, American Nuclear Society, Hinsdale. Ill., 1967.

9. Stiegler, J. O., Farrell, K., and McCoy, H. E., "Stress-Induced Growth of Gas Bubbles in Solids," *Journal of Nuclear Materials*, 25 (3), 340-343 (1968).

10. Farrell, K., Houston, J. T., and Chumley, J. W., "Hot Cracking in Fusion Welds in Tungsten," submitted to WELDING JOURNAL for publication.